Ca^{2+}-dependent and -independent mechanisms of calmodulin nuclear translocation

Richard Thorogate and Katalin Török*

Department of Basic Medical Sciences, St Georges Hospital Medical School, Cranmer Terrace, London, SW17 0RE, UK
*Author for correspondence (e-mail: k.torok@sghms.ac.uk)

Accepted 24 August 2004
Journal of Cell Science 117, 5923-5936 Published by The Company of Biologists 2004
doi:10.1242/jcs.01510

Summary

Translocation from the cytosol to the nucleus is a major response by calmodulin (CaM) to stimulation of cells by Ca^{2+}. However, the mechanisms involved in this process are still controversial and both passive and facilitated diffusion have been put forward. We tested nuclear translocation mechanisms in electroporated HeLa cells, rat cortical neurons and glial cells using novel calmodulin and inhibitor peptide probes and confocal microscopy. Passive diffusion of calmodulin across the nuclear membrane was measured in conditions in which facilitated transport was blocked and was compared to that of a similarly sized fluorescein-labeled dextran. Wheat germ agglutinin, which blocks facilitated transport but not passive diffusion, inhibited the nuclear entry of both wild-type and Ca^{2+}-binding-deficient mutant calmodulin both in low and elevated [Ca^{2+}]. Ca^{2+}-dependent nuclear translocation was prevented by a membrane-permeant CaM inhibitor, the mTrp peptide, which indicated that it was specific to Ca^{2+}/CaM. Diffusion of free CaM and Ca^{2+}/CaM was considerably slower than the observed nuclear translocation by facilitated transport. Our data show that the majority of CaM nuclear entry occurred by facilitated mechanisms in all cell types examined, in part by a Ca^{2+}-independent and in part by a Ca^{2+}-dependent translocation mechanism.

Key words: CaM, Nucleus, Transport, Calcium, NLS

Introduction

Calmodulin (CaM) is a ubiquitous Ca^{2+}-binding protein that exists as a monomer of 16.8 kDa and belongs to the EF-hand homolog family, which includes 160 different Ca^{2+} binding proteins (Persechini et al., 1989; Pruschy et al., 1994). CaM can transduce a Ca^{2+} signal into a cellular response to regulate processes in the cytoplasm and in the nucleus such as cytoskeletal structure changes, metabolic activity, gene expression, synaptic plasticity and nitric oxide synthesis (Mayer et al., 1992; Teruel et al., 2000; Deisseroth et al., 2003). During cell division, following nuclear entry, CaM remains associated with the mitotic apparatus (Török et al., 1998a; Li et al., 1999; Yu et al., 2004). A high concentration of CaM has been found in the nucleus of all cell types and it is believed that CaM functions through regulating the activities of CaM-binding proteins located there at high concentration (Bachs et al., 1994).

The mechanism of molecular transport into the nucleus is not fully understood, but is thought to occur via the nuclear pore complex (NPC), which regulates nucleocytoplasmic trafficking of ions, proteins and RNA in eukaryotic cells (Liao et al., 1999; Wang and Clapham, 1999). Molecular transport can occur via active or passive mechanisms depending on the size of the molecule, requirements for energy and the presence of a nuclear localization signal (NLS) (Perez-Terzic et al., 1999). It has been reported that molecules no larger than 45-60 kDa (depending on the cell type) can transverse the NPC by passive diffusion, whereas larger molecules that possess an NLS sequence require energy-dependent multi-step processes to enter and exit the nucleus (Allen et al., 2000; Perez-Terzic et al., 1999; Weiss, 1998). For a detailed review of NLS-dependent transport see Allen et al. (Allen et al. 2000). Although the translocation of NLS-containing proteins has been extensively studied, little is known about the mechanisms that regulate passive diffusion. However, pore permeability can be regulated by emptying the Ca^{2+} stores of the endoplasmic reticulum (ER), which then prevents the passive diffusion of molecules larger than 10 kDa (Greber and Gerace, 1995; Lee et al., 1998; Perez-Terzic et al., 1999; Strübing and Clapham, 1999). The blockade of medium-sized molecules can be reversed by adding Ca^{2+} and ATP to a bath, containing isolated nuclei (Wang and Clapham, 1999). Depletion of Ca^{2+} is thought to be sensed by the nucleoporin gp210 that, through its large lumenal domain, containing several putative Ca^{2+}-binding sites, could induce conformational changes on the NPC (Perez-Terzic et al., 1997). According to Greber and Gerace, NLS-signal-mediated transport cannot occur when Ca^{2+} is released from intracellular stores (Greber and Gerace, 1995). However, Strübing and Clapham found that in HM1 cells (a human embryonic kidney cell line) ER-store depletion by carbachol, thapsigargin, ionomycin or 1,2-bis-(*o*-aminophenoxy) ethane-*N,N,N′,N′*-tetraacetic acid-acetoxymethyl ester (BAPTA-AM) had no effect on the nuclear import of the NLS-containing mitogen-activated protein (MAP) kinase-activated protein kinase 2 (MK2) (Strübing and Clapham, 1999).

Previous studies, investigating how CaM enters the nucleus have so far produced conflicting data. CaM lacks an obvious NLS motif and, because of its small size, import could occur by passive diffusion, depending on the diameter of the nuclear

pores. In permeabilized or intact A7r5 cells, CaM translocation into the nucleus is not blocked by wheat germ agglutinin (WGA) or chilling, and does not require cytosolic factors or an ATP regenerating system (Liao et al., 1999). Also, nuclear accumulation of CaM is blocked by a CaM antagonist peptide, M13, and the amount of CaM in the nucleus increases with increasing concentrations of free Ca^{2+}. CaM accumulation in the nucleus was also shown to be similar to the rate of uptake of a 20-kDa fluorescein-dextran (FL-dextran), consistent with a first order process. It was therefore concluded that nuclear entry is owing to passive diffusion and the steady state concentration of CaM in the nucleus depends on both the intracellular concentration of free Ca^{2+} and the relative concentration and affinity of CaM-binding proteins (Liao et al., 1999). However, Pruschy et al. found that CaM import is inhibited by WGA and chilling, but that ATP depletion did not affect nuclear uptake in PtK1 cells and this indicated a facilitated but not active transport mechanism (Pruschy et al., 1994). It was therefore suggested that CaM could be in a complex with a CaM-binding protein that was too large to enter the nucleus by diffusion. This idea was supported by evidence gained from experiments in smooth muscle cells that only 5% of total endogenous CaM was free, even at resting intracellular Ca^{2+}, and the observed hindered diffusion of CaM was owing to a pool of CaM that was tightly bound to a target. Upon elevation of intracellular Ca^{2+} levels, a large portion of CaM was released and was thought to bind again, this time to Ca^{2+}-dependent CaM binding sites in the nucleus (Luby-Phelps et al., 1995). Diesseroth et al. demonstrated that, in hippocampal neurons, brief bursts of activity caused fast translocation (within approximately 1 minute) of CaM from the cytoplasm to the nucleus (Diesseroth et al., 1998). Rapid chilling abolished this rapid translocation of CaM, although a persistent and slow leakage of CaM into the nucleus was observed for a long time after the stimulus. It was concluded that CaM translocation into the nucleus was not merely by diffusion but facilitated. Mermelstein et al. suggested that CaM interacts with Ca^{2+}/CaM-dependent protein kinase kinase (CaMKK) for translocation (Mermelstein et al., 2001). In hippocampal neurons, the CaM kinase inhibitor KN-93 blocked CaM translocation into the nucleus, suggesting that CaM kinases or an isoform of CaMKK is required for CaM translocation. Furthermore, translocation of a fluorescently tagged CaM was prevented by fusing it with M13 peptide. This further suggested that CaM requires a Ca^{2+}-dependent association with an endogenous CaM-binding protein to allow CaM translocation into the nucleus.

First, we used electroporated HeLa, cortical glial and neuronal cells to study the permeability of the nuclear pores using differently sized FL-dextrans. Second, we investigated CaM translocation into the nucleus and binding to nuclear targets in HeLa cells using a novel rhodamine-labeled CaM probe. We demonstrate that CaM entry into the nucleus occurs via two separate mechanisms, of which one is Ca^{2+}-dependent and one is Ca^{2+}-independent.

Materials and Methods

CaM expression and purification

The expression vector $pAED_4$, containing CaM cDNA of human liver subcloned in the restriction sites *Nde*I for 5′ and *Pst*I for 3′, was a kind gift from S. Marston (Imperial College, London, UK). CaM was expressed using standard procedures and purified as described by Török and Trentham (Török and Trentham, 1994). The purified CaM was desalted on a Sephadex PD-10 column (Amersham Biosciences) and then lyophilized. The typical yield was 20 mg/l culture. A mutant form of CaM (CaM1234) with mutations in the four Ca^{2+}-binding lobes that prevent Ca^{2+}-binding (Kasri et al., 2003), was prepared like CaM and labeled with 6ROX similarly to wild-type CaM (data not shown).

CaM labeling with 6ROX

Human liver CaM expressed in *Escherichia coli* was labeled at a concentration of 1 mg/ml (60 μM) in 200 mM Tris-HCl pH 8.5, containing 20 mM $CaCl_2$ with 120 μM 6-carboxy-X-rhodamine, succinimidyl ester (6ROX, SE) (Molecular Probes). Labeling was carried out in the dark for 1 hour at 22°C for the formation of Lys75-6-carboxy-X-rhodamine-labeled CaM (6ROX-CaM) and the reaction was terminated by gel filtration on a PD10 column equilibrated with H_2O. Purification by HPLC was carried out as described in Török et al. with absorption measured at 215 nm and fluorescence monitored at 568 nm excitation and 602 nm emission (Török et al., 2002). In HPLC analysis the second of two fluorescent peaks corresponded to Lys75-labeled 6ROX-CaM. Absorption was measured at 575 nm and the extinction coefficient ε_o for 6ROX-CaM was taken as 82,000 $M^{-1}cm^{-1}$ (Molecular Probes).

6ROX-CaM tryptic digest

Digestion mixtures consisted of 100 mM NH_4HCO_3 pH 9.0, 2 mM EGTA, 1 mg/ml 6ROX-CaM and 10 μg/ml trypsin. All digestions were performed at 37°C for 20 hours.

Matrix-assisted laser desorption and ionization time-of-flight (MALDI-TOF) mass spectrometry analyses

Sinapinic acid was used as a matrix for the ionisation of 6ROX-CaM. α-cyano-4-hydroxycinnamic acid was used as a matrix for the ionisation of polypeptides from the tryptic digest of 6ROX-CaM. A saturated solution of 10 mg α-cyano-4-hydroxycinnamic acid in 700 μL acetonitrile and 300 μL 0.1% TFA in an amber eppendorf and left to settle under gravity. Samples were desalted using C_{18} ZipTips pipette tips (Millipore) and 0.5 μl of the appropriate matrix was loaded onto the MALDI-TOF analysis plate with 10 pmol 6ROX-CaM or 5 pmol of peptide sample. Samples were analysed on an Axima-CFR MALDI-TOF mass spectrometer (Kratos Analytical); the system was calibrated with angiotensin II (1046.2 Da) for tryptic digest analysis and human liver CaM (16706.4 Da) for undigested CaM analysis.

Fluorescence measurements

The fluorescence of 6ROX-CaM was measured spectro-fluorometrically (SLM Aminco®) upon titration of free Ca^{2+}. Excitation was set to 568 nm and emission was measured at 605 nm. Measurements were performed in a solution of 50 mM 2-(*N*-morpholino) ethanesulfonic acid K^+ salt (K-MES) pH 7.0, 100 mM KCl, 2 mM $MgCl_2$ and 5 mM EGTA at 21°C, containing 100 nM 6ROX-CaM. Tyr fluorescence of 100 nM unlabeled CaM and CaM1234 was measured in the same buffer. Excitation was set to 278 nm and emission was measured at 305 nm. [Ca^{2+}] concentrations were calculated as described before (Tzortzopoulos et al., 2004).

Peptide inhibitors

A cell permeant CaM-binding peptide based on the acetylated Trp peptide (Ac-RRKWQKTGHAVRAIGRL-$CONH_2$) (Török and

Trentham, 1994; Török et al., 1998a; Török et al., 1998b) was generated by N-terminal myristoylation instead of acetylation. This myristoylated peptide (mTrp) was HPLC-purified to homogeneity and its K_d for 2-chloro-(ε-amino-Lys75)[6-4-(*N,N*-diethhylamino)phenyl]-1,3,5-triazin-4-yl-CaM (TA-CaM) was determined by stopped-flow kinetic experiments in a Hi-Tech PQ/SF-51MX multimixing stopped-flow spectrofluorimeter (Hi-Tech Scientific, UK) in the solution conditions above with the exception of EGTA being replaced by 100 μM $CaCl_2$.

A cell permeant analogue of the Ca^{2+}/CaM-dependent protein kinase II (CaMKII) inhibitor AIP, myristoyl-AIP (mAIP, myristoyl-NKKALRRQGAVDAL-OH) (Ishida et al., 1995) from Calbiochem was also tested as an inhibitor of CaM nuclear translocation to see if CaMKII was involved in the translocation mechanism.

cAMP phosphodiesterase (PDE) assays

Unlabeled, human liver CaM that had been expressed in *E. coli*, 6ROX-CaM and 6ROX-CaM1234 were measured and their activating effects on CaM-free cAMP PDE of the heart were compared. One activator unit of CaM is defined as the amount of CaM that is necessary to raise the activity of 3 mU of Ca^{2+}-free PDE to 50% of its maximum at CaM saturation. Measurement value was the decrease in adenosine extinction at 265 nm. For detailed methodology see Török et al. (Török et al., 1998b).

HeLa cell culture

HeLa cells (ATCC lot number 2056308) were cultured in minimum essential medium (MEM) (Sigma) supplemented with 2 mM L-glutamine, 1.5 g/l sodium bicarbonate, 0.1 mM non-essential amino acids, 1 mM sodium pyruvate, 100 U/ml penicillin and 100 μg/ml streptomycin and 10% heat inactivated fetal bovine serum. Cells were maintained in a humidified atmosphere of 5% CO_2 at 37°C and were passaged every 3 days. For imaging, cells were grown on 35×10 mm culture dishes and synchronized with 10 ng/ml aphidicolin.

Cortical neuron and glial cell culture

Cortical neurons and glial cells were prepared from neonatal rat pups (Wistar) using a papain based dissociation method. Cells were grown on 25 mm glass coverslips coated with 10 μg/ml poly-L-lysine and 1 μg/ml laminin and incubated in a humidified atmosphere (95% air and 5% CO_2). Cells were grown in basal medium Eagle (BME) with Earle's salts, without glutamine (Gibco BRL, UK) without L-glutamine and supplemented with Earle's salts, N_2 supplement, 10% horse serum, 20 mM glucose, 100 U/ml penicillin and 100 μg/ml streptomycin. Cells were used for imaging after 6-10 days of culture.

Electroporation

Cells were loaded by electroporation as described before (Török et al., 2002). For a detailed review on electroporation see Teruel and Meyer (Teruel and Meyer, 1997). HeLa, glial and neuronal cells were washed and kept in electroporation buffer, containing 135 mM NaCl, 5 mM KCl, 1.3 mM $MgSO_4$, 10 mM glucose, 2 mM EGTA and 20 mM HEPES (pH 7.4) for 15 minutes. Just before electroporation, cells were put into 1 ml electroporation buffer to which 0.5 μM tetrodotoxin (TTX) was added and cells were electroporated with 6ROX-CaM, 6ROX-CaM1234 and/or 4.3-77 kDa FL-dextrans (Molecular Probes) (estimated final concentration 4 μM) or fluo-4 (Molecular Probes) (estimated final concentration 3 μM) by applying two 25 ms 105 V cm^{-1} pulses of opposite polarity. Cells were then washed and put back into electroporation buffer for 15 minutes before imaging.

To inhibit facilitated transport, cells were electroporated with WGA to an estimated final concentration of 20 μg/ml. In CaM inhibitory experiments, 10 μM mTrp peptide was added to electroporation buffer and the cells were incubated for 15 minutes before stimulation

Cell stimulation

To observe Ca^{2+}-dependent CaM translocation, cells that had been kept in 2 mM EGTA were stimulated by the addition of 2.1 mM Ca^{2+} to the external medium. Intracellular Ca^{2+} transients were induced in HeLa cells by the addition of 50 μM histamine to the external medium (Bootman et al., 1997).

Where specified, as a means of stimulation, 4 mM Ca^{2+} was added to the cells in electroporation buffer to give a final concentration of 2 mM Ca^{2+} and observed for the specified amount of time up to 1 hour.

Confocal imaging

Cells were imaged on a Leica SP system with a 63×0.9 water immersion lens, using a 568 nm krypton laser to excite 6ROX-CaM and a 488 nm argon laser to excite fluo-4 and FL-dextrans. Images were taken at 7-second intervals for 1400 seconds at 22°C in electroporation buffer (SB) and had a box size of 512×512 pixels.

Statistics

Results are expressed as the mean±s.e.m. and n=number of experiments. All statistical analysis was performed using the parametric test ANOVA-one way. Significant difference was accepted at $P<0.01$.

Results

Characterization of the 6ROX-CaM, 6ROX-CaM1234 and mTrp probes

Human liver CaM expressed in *E. coli* was labeled with 6-ROX, in conditions that had previously been used to generate Lys75-labeled TA-CaM and FL-CaM (Török and Trentham, 1994; Török et al., 1998a; Török et al., 2002). The reagent 6ROX was chosen to simultaneously image changes in intracellular [Ca^{2+}] by fluo-4 and CaM. Additionally, 6ROX was expected to be more photostable than fluorescein, which had previously been used for FL-CaM and is excited by visible, rather than UV light. MALDI-TOF analysis of HPLC-purified 6ROX-CaM (Fig. 1A) showed that labeling occurred at a single site (Fig. 1B). Analysis of the tryptic digest of 6ROX-CaM revealed that the Lys75-Lys77 and the Lys75-Arg86 peptides were bound to 6ROX (Fig. 1C,D). Post-source decay sequence analysis identified Lys75 as the labeled residue (data not shown) as observed previously for TA-CaM and FL-CaM. No other masses were found in the 6ROX-CaM tryptic digests to suggest that 6ROX was bound to any other Lys residues. Similar results were obtained for the CaM mutant 6ROX-CaM1234, in which labeling also occurred at Lys75 (data not shown).

PDE was activated by 6ROX-CaM with similar K_m and V_{max} values as unlabeled CaM expressed in *E. coli*. The K_m for CaM was 6.5±0.7 nM and 8.3±0.9 nM for 6ROX-CaM (Fig. 1E,F). 6ROX-CaM1234, however, did not activate PDE. 6ROX-CaM showed a small (6 nm) hypsochromic shift in emission (604 to 598 nm) upon the increase of free Ca^{2+} to 1.74 μM, fluorescence was increased 1.46-fold (Fig. 1G). The addition of more Ca^{2+} had no further effect on the fluorescence, which reduced to base level again upon the

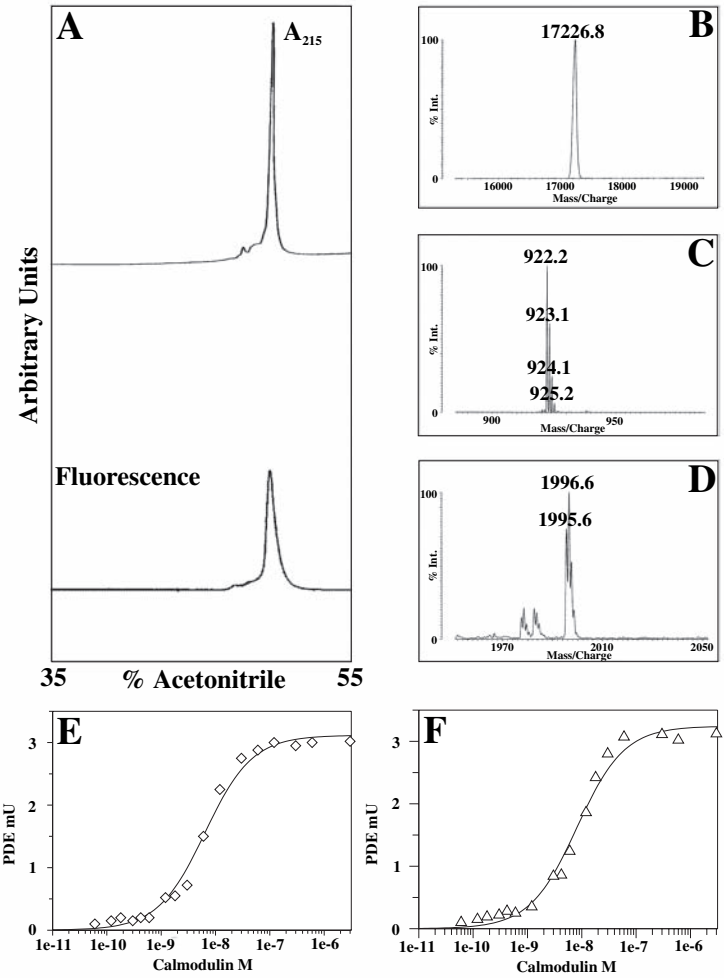

Fig. 1. Characterization of 6ROX-CaM (A) HPLC analysis of 6ROX-CaM purified by a Vydac reverse-phase C_8 column (4.6×150 mm). The chromatogram shows a single absorbance peak at 215 nm with a corresponding fluorescent peak measured at an excitation wavelength of 568 nm and an emission wavelength of 602 nm. (B) MALDI-TOF mass spectroscopy of undigested 6ROX-CaM. Obtained was an average mass of 17226.8 Da [average theoretical mass, 17223.1 Da (6ROX reacted =516.7 Da + 16706.4 Da for human liver CaM expressed in *E. coli*)]. (C,D) MALDI-TOF mass spectroscopy of the labeled peptides of 6ROX-CaM digested with trypsin. Peptide 75-77 (theoretical monoisotopic mass, 405.2 Da) bound to the 6ROX probe (monoisotopic mass, 922.2 Da; theoretical monoisotopic mass, 922.3 Da) (C). Peptide 75-86 (theoretical monoisotopic mass, 1479.7 Da) bound to the 6ROX probe (monoisotopic mass, 1995.6 Da; theoretical monoisotopic mass, 1997.3 Da) (D). (E,F) Activation of PDE by unlabeled CaM (◇) and 6ROX-CaM (△). K_m was 6.5 (±0.7) nM for CaM and 8.3 (±0.9) nM for 6ROX-CaM. (G) Fluorescent properties of 6ROX-CaM. Ca^{2+}-titration of 100 nM 6ROX-CaM was carried out in 5 mM EGTA, 100 mM KCl, 2 mM $MgCl_2$ and 50 mM K-MES, pH 7.0 at 21°C. Emission was corrected for buffer. Ca^{2+} concentrations were in the order of rising relative fluorescence: 0.4 nM, 0.29 μM, 0.652 μM and 1.74 μM. (H) The effect of Ca^{2+}-binding on tyrosine fluorescence of WT-CaM (+) and CaM1234 (△). Fluorescence was monitored at an excitation wavelength of 278 nm and an emission wavelength of 305 nm. (Ii-Iiii) Measurement of the K_d of mTrp peptide binding to TA-CaM by stopped-flow kinetics. (Ii) Association kinetics. 12 nM TA-CaM was rapidly mixed with 175 nM mTrp peptide (concentrations in mixing chamber are given) in the same solution conditions as the other fluorescent measurements were made. The biphasic fluorescence increase was fitted by two exponentials at 45 seconds^{-1} (0.75) and 3.8 seconds^{-1} (0.25). (Iii) Observed rates of association are plotted as a function of mTrp peptide concentration. The gradient (◆) was 2.2×10^8 M^{-1} seconds^{-1}. The rate of the slow step saturated at 3.8 seconds^{-1} (●). (Iiii) Ca^{2+}/TA-CaM.mTrp complex dissociation kinetics. Ca^{2+}/TA-CaM was displaced from the complex by an excess of 2 μM unlabeled CaM. The rate constant of dissociation was 0.003 seconds^{-1}.

addition of 4 mM EGTA (data not shown). Unlabeled CaM showed a 3-fold increase in the Tyr fluorescence upon increasing [Ca^{2+}] – with a midpoint of fluorescence enhancement at 535 nM and a Hill coefficient of n=2 – whereas unlabeled CaM1234 showed no significant increase, consistent with its inability to bind Ca^{2+} (Fig. 1H).

The previously described Trp peptide (Török and Trentham, 1994; Török et al., 1998a; Török et al., 1998b) was myristoylated at the N-terminus to make it membrane permeant. The Ca^{2+}/CaM-binding properties of mTrp peptide were determined by stopped-flow fluorimetry using TA-CaM. Similarly to Trp peptide, mTrp had a high affinity, with a K_d of 15 pM for Ca^{2+}/TA-CaM (Fig. 1I).

Depletion and refilling of intracellular Ca^{2+} stores

The nuclear pore size has been reported to be affected by the level of Ca^{2+} within the intracellular Ca^{2+} stores (Perez-Terzic et al., 1997). Therefore, we examined the state of the Ca^{2+} stores under our conditions. HeLa cells were loaded with 3 μM of the cell permeant fluo-4AM ester (F14217 Molecular Probes) for 15 minutes and stimulated with 50 μM histamine under a range of extracellular and intracellular Ca^{2+} conditions. In the presence of 2 mM extracellular Ca^{2+}, histamine induced Ca^{2+} oscillations, initially occurred at 40-second intervals whose frequency and intensity decreased over time (Fig. 2A). Cells incubated with 2 mM extracellular EGTA and stimulated after 15 minutes with 50 μM histamine, also showed oscillations that initially started at 40-second intervals but decreased in frequency and intensity. However, under the above conditions, oscillations ceased more rapidly than in the presence of 2 mM extracellular Ca^{2+} (Fig. 2B) because refilling of intracellular stores required Ca^{2+} influx through plasma membrane ion channels. Cells that had been electroporated with fluo-4 while 2 mM EGTA was present in the medium showed no response to 50 μM histamine. This lack of response might indicate that, electroporation of cells while EGTA is present in the medium can result in either the depletion of Ca^{2+}stores or in the buffering of released Ca^{2+} by EGTA entering the cell during electroporation (Fig. 2C). Cells stimulated with 2.1 mM Ca^{2+} after they had been loaded with fluo-4, showed a large single transient. Addition of 50 μM histamine after this transient had diminished caused another single, small Ca^{2+} transient, typically after about 20-25 minutes (n=3), indicating that the intracellular stores had partially refilled with Ca^{2+} (Fig. 2D).

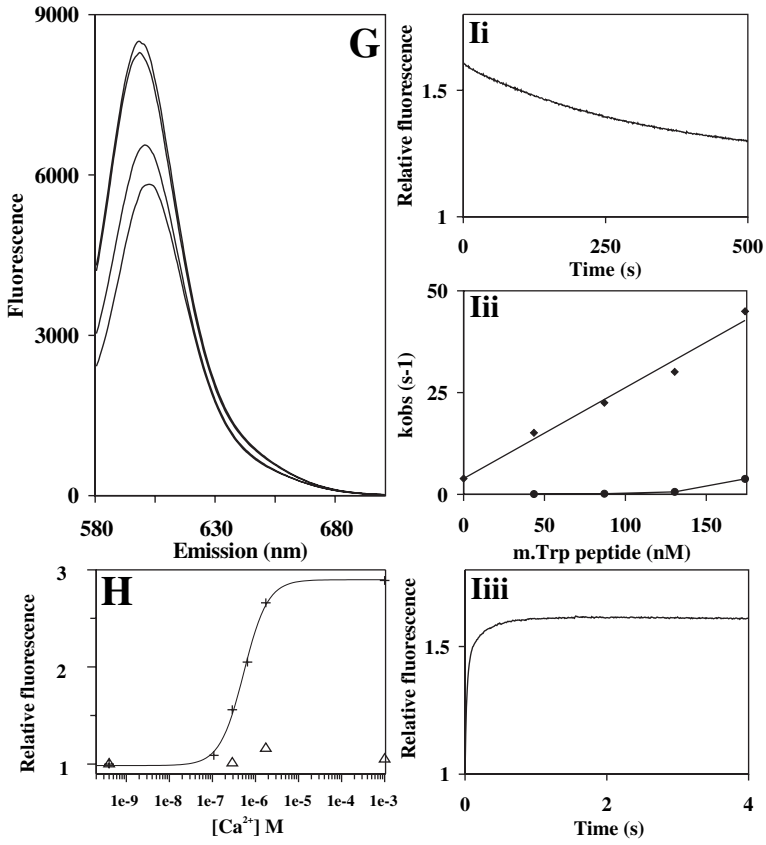

Ca^{2+} stimulation of HeLa cells

An intracellular Ca^{2+} transient was generated by the addition of free Ca^{2+} to the extracellular solution as demonstrated above (Fig. 2). Upon addition of 2.1 mM Ca^{2+}, fluo-4 fluorescence was increased by 10.2±1.2 (n=16) in the nucleoplasm of the cells. Fluo-4 fluorescence was also higher in the nucleoli and other nuclear structures. 1300 seconds after Ca^{2+} stimulation, the fluorescence-level dropped to 2.7±0.3 above the original level.

FL-dextran diffusion through the nuclear pores

To measure diffusion from the cytoplasm into the nucleus, we used 19.5-kDa FL-dextran, which is similar in size to CaM, and measured the change in the ratio of nucleoplasmic to cytoplasmic fluorescence (F_{np}:$F_{cytoplasm}$). Measurements were carried out over 1 hour in glial cells that had been kept in 2 mM EGTA and also in glial cells to which 2.1 mM Ca^{2+} was added. In 2 mM EGTA only, the change of the F_{np}:$F_{cytoplasm}$ ratio was 0.003±0.0002/minute (n=4) (Fig. 3A). However, after the addition of 2.1 mM Ca^{2+}, the change of ratio increased to 0.008±0.001/minute (n=4) (Fig. 3A). This indicated that the higher intracellular Ca^{2+} concentration was causing the nuclear pores to be in a more open conformation.

Distribution of FL-dextrans in HeLa cells

We examined the permeability of the nuclear pores with 4.3-, 9.5-, 19.5-, 40- and 77-kDa FL-dextrans, by observing their distribution at low intracellular [Ca^{2+}] and after stimulation by Ca^{2+}. HeLa cells in EGTA that had been electroporated with fluorescent dextrans were imaged after 15 minutes, cells in 2 mM free Ca^{2+} were imaged after 1 hour. Also, cells were electroporated with WGA to determine whether it has any effect on the passive transport of FL-dextrans in the presence and absence of intracellular Ca^{2+}.

In the case of 4.3-kDa FL-dextran, the F_{np}:$F_{cytoplasm}$ ratio of cells in 2 mM EGTA (4.3 kDa: 1.23±0.1, n=5) (Fig. 3B) was not significantly different compared with cells in 2 mM Ca^{2+} (4.3 kDa: 1.3±0.03, n=6) (Fig. 3G). Thus, this small dextran was able to freely enter the nucleus, even at the more-closed state of the nuclear pores. However, significantly different F_{np}:$F_{cytoplasm}$ ratios were seen between cells in 2 mM EGTA and cells in 2 mM Ca^{2+}, when 9.5-, 19.5- and 40-kDa FL-dextran was used. The use of 9.5-, 19.5- and 40-kDa FL-dextran, respectively, gave ratios of 1.0±0.03 (n=6), 0.56±0.03 (n=8) and 0.11±0.01 (n=7) for cells in 2 mM EGTA (see Fig. 3C-E), and increased ratios of 1.28±0.05 (n=6), 1.03±0.02 (n=7) and 0.39±0.02 (n=6) for cells kept in 2 mM Ca^{2+} for 1 hour (see Fig. 3B, Table 1).

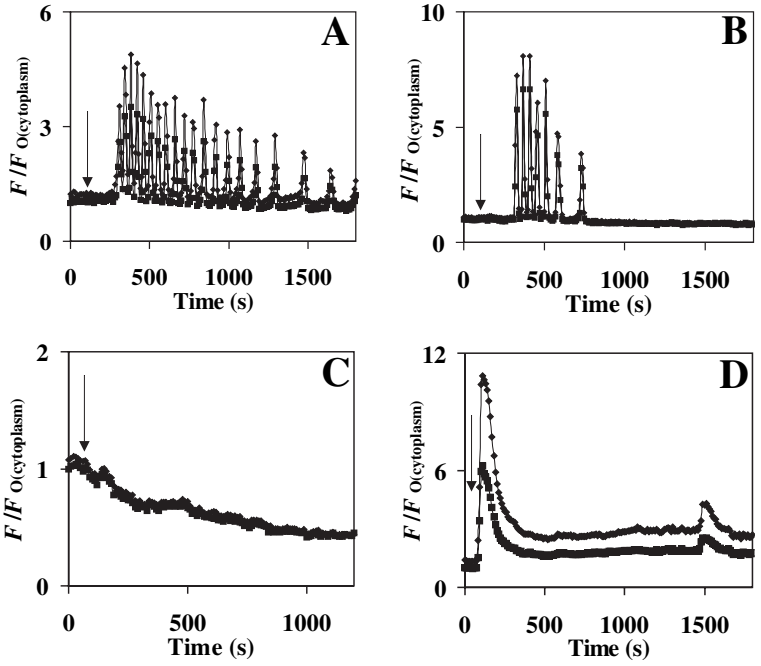

Fig. 2. Effect of electroporation on intracellular Ca^{2+} stores in HeLa cells. Graphs show normalized fluorescence ($F/F_{O(cytoplasm)}$). (A) Cells in 2 mM extracellular Ca^{2+} were loaded with fluo-4AM and stimulated with 50 μM histamine at t_{100} seconds. (B) Cells in 2 mM EGTA were incubated for 15 minutes and stimulated with 50 μM histamine at t_{100} seconds. (C) Cells in 2 mM EGTA were electroporated with fluo-4 and stimulated with 50 μM histamine at t_{100} seconds. (D) Cells electroporated in 2 mM EGTA were stimulated with 2.1 mM Ca^{2+} at t_{30} seconds and then stimulated with 50 μM histamine t_{1000} seconds. Arrows indicate addition of 50 μM histamine.

The addition of 10 μM BAPTA-AM before electroporating cells with 19.5 kDa dextran did not alter the F_{np}:$F_{cytoplasm}$ ratios further; they were 0.54±0.03 (n=5) in BAPTA-AM, compared with 0.56±0.03 (n=8) of cells in 2 mM EGTA only (Fig. 3B). The 77-kDa FL-dextran was excluded from the nucleus regardless of the [Ca^{2+}]. Cells in 2 mM Ca^{2+} had a F_{np}:$F_{cytoplasm}$ ratio of 0.1±0.02 (n=6), whereas cells kept in EGTA had a ratio of 0.14±0.05 (n=6) (Fig. 3G, Table 1). WGA, which is known to block NLS-facilitated nuclear import but not passive diffusion (Dabauvalle et al., 1988) did not significantly inhibit the diffusion of any FL-dextran in high or low [Ca^{2+}].

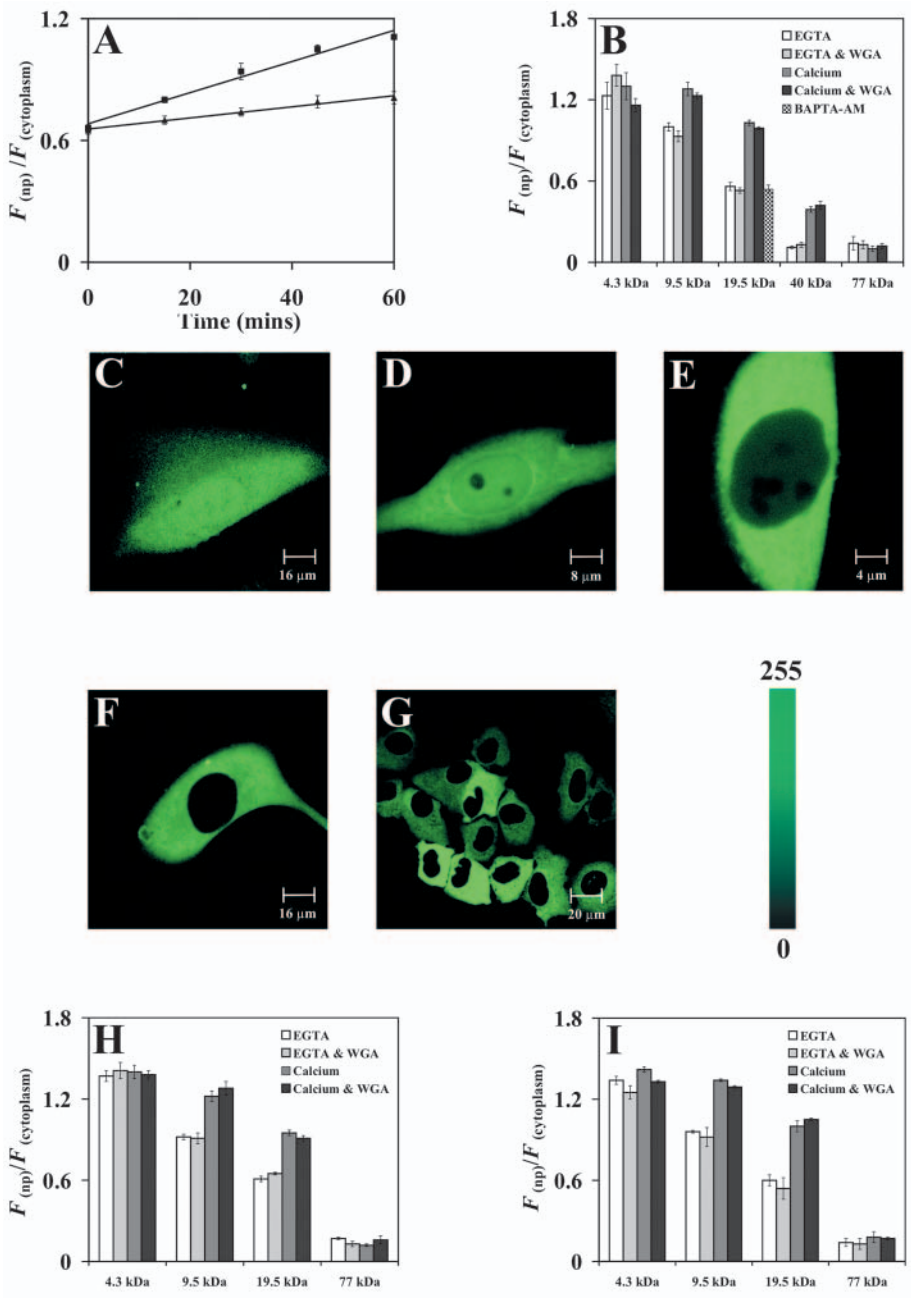

Fig. 3. FL-dextran distribution in electroporated cells. (A-G) HeLa cells. Passive diffusion rates of 19.5 kDa FL-dextran. Cells were electroporated with 19.5 kDa FL-dextran and nucleoplasmic to cytoplasmic fluorescence ratio ($F_{np}/F_{cytoplasm}$) was monitored for 60 min in 2 mM EGTA (▲) or 2.1 mM Ca^{2+} containing electroporation buffer (■). (B) Graphs show $F_{np}/F_{cytoplasm}$ ratios of cells in the specified conditions. Order of groups of columns from left to right. Cells in 2 mM EGTA for 15 minutes; cells in 2 mM EGTA and 20 μg/ml WGA for 15 minutes; addition of 2 mM Ca^{2+} for 1 hour; addition of 2 mM Ca^{2+} for 1 hour with 20 μg/ml WGA electroporated; addition of 10 μM BAPTA-AM before electroporation in 2 mM EGTA. (C-G) Confocal images of 4.3-, 9.5-, 19.5-, 40- and 77-kDa FL-dextrans, respectively, in HeLa cells in 2 mM EGTA imaged 15 minutes after electroporation. (H,I) Dextran distributions in cortical glial cells (H) and cortical neurons (I). Order of groups of columns from left to right: cells in 2 mM EGTA for 15 minutes; cells in 2 mM EGTA and 20 μg/ml WGA for 15 minutes; addition of 2 mM Ca^{2+} for 1 hour; addition of 2 mM Ca^{2+} for 1 hour with 20 μg/ml WGA electroporated.

Distribution of FL-dextrans in cortical glial cells

Glial cells were electroporated with 4.3-, 9.5-, 19.5- or 77-kDa FL-dextrans and 2 mM EGTA. When electroporated with the 4.3-kDa FL-dextran there was no significant difference in the F_{np}:$F_{cytoplasm}$ ratio of cells in 2 mM EGTA (1.34±0.03, n=6) compared with cells in 2 mM Ca^{2+} for 1 hour (1.42±0.04, n=4) (Fig. 3H). However, 9.5- and 19.5-kDa FL-dextran showed significant increases. Ratios, using 9.5- and 19.5-kDa FL-dextran, respectively, were 0.96±0.05 (n=7) and 0.6±0.02 (n=5) in cells kept in 2 mM EGTA, and 1.34±0.04 (n=5), 1±0.04 (n=5) in cells kept in 2 mM Ca^{2+} for 1 hour (see Fig. 3H). 77-kDa FL-dextran was excluded from the nucleus regardless of the [Ca^{2+}]. For cells kept in 2 mM Ca^{2+}, the F_{np}:$F_{cytoplasm}$ ratio was 0.18±0.01 (n=7), whereas for cells in EGTA it was 0.14±0.01 (n=8) (Fig. 3H, Table 1). WGA did not significantly inhibit the diffusion of any FL-dextran in high or low [Ca^{2+}].

Distribution of FL-dextrans in cortical neurons

Neurons were electroporated with 4.3-, 9.5-, 19.5- or 77-kDa FL-dextrans and 2 mM EGTA. When electroporated with the 4.3-kDa FL-dextran, there was no significant difference in the F_{np}:$F_{cytoplasm}$ ratio of cells in 2 mM EGTA (1.37±0.04, n=6) compared with cells in 2 mM Ca^{2+} for 1 hour (1.4±0.05, n=4) (Fig. 3I). However, 9.5- and 19.5-kDa FL-dextran showed significant differences in the F_{np}:$F_{cytoplasm}$ ratios of cells in 2 mM EGTA compared with cells in 2 mM Ca^{2+} for 1 hour. Ratios, using 9.5- and 19.5-kDa FL-dextran, respectively, were 0.92±0.02 (n=6) and 0.61±0.02 (n=5) for cells in 2 mM EGTA and 1.22±0.04

(n=5) and 0.95±0.02 (n=5) for cells in 2 mM Ca^{2+} (Fig. 3I). 77-kDa FL-dextran was excluded from the nucleus regardless of the Ca^{2+}conditions. In 2 mM Ca^{2+} the F_{np}:$F_{cytoplasm}$ ratio was 0.12±0.01 (n=6), whereas the ratio in EGTA was 0.17±0.01 (n=6) (Fig. 3I, Table 1). WGA did not significantly inhibit the diffusion of any FL-dextran in high or low [Ca^{2+}].

Table 1. Ratios of F_{np}:$F_{cytoplasmic}$ of differently sized FL-dextrans in HeLa, glial and neuronal cells

Cell type	Dextran (size in kDa)	Ratio in EGTA	Ratio in Ca^{2+}	Ratio increase
HeLa cells	4.3	1.23±0.1	1.30±0.03	1.1
	9.5	1.00±0.03	1.28±0.05	1.3
	19.5	0.56±0.03	1.03±0.02	1.8
	40	0.11±0.01	0.39±0.02	3.6
Glial cells	4.3	1.34±0.03	1.42±0.04	1.1
	9.5	0.96±0.05	1.34±0.04	1.4
	19.5	0.60±0.02	1±0.04	1.7
	77	0.14±0.01	0.18±0.01	1.3
Neurons	4.3	1.37±0.04	1.40±0.05	1.0
	9.5	0.92±0.02	1.22±0.04	1.3
	19.5	0.61±0.02	0.95±0.02	1.6
	77	0.17±0.01	0.12±0.01	0.7

Ratios of F_{np}:$F_{cytoplasmic}$ of differently sized FL-dextrans in HeLa cells, glial cells and cortical neurons in the presence of 2 mM EGTA and 2 mM free extracellular Ca^{2+} in the medium. Cells were electroporated with the specified dextran as described in Materials and methods and fluorescence imaging was carried out 15 minutes after electroporation of cells in medium containing 2 mM EGTA (concentration of free Ca^{2+} in the medium, <10 nM) and 1 hour after stimulation of cells with 4 mM Ca^{2+} (final concentration of free Ca^{2+}, 2 mM).

The above results show that similar changes of F_{np}:$F_{cytoplasm}$ ratios are obtained in HeLa cells, glial cells and neurons. When cells had been electroporated with 9.5- and 19.5-kDa FL-dextrans and were left in high [Ca^{2+}] for 1 hour, F_{np}:$F_{cytoplasm}$ ratios were significantly different owing to different diffusion rates of the differently sized dextrans into the nucleus. In all cell three cell types, the 9.5-, 19.5- and 40-kDa FL-dextrans showed significant differences in F_{np}:$F_{cytoplasm}$ ratios in cells kept in EGTA and cells kept in Ca^{2+}, providing evidence that Ca^{2+} increased the nuclear pore size.

Ca^{2+}-independent nuclear translocation of 6ROX-CaM

Upon loading the cells with 6ROX-CaM in 2 mM EGTA, the F_{np}:$F_{cytoplasm}$ ratios for glial, neuronal and HeLa cells were 1.26±0.03 (n=10), 0.97±0.02 (n=4) and 1.18±0.03 (n=19), respectively (Fig. 4A). These ratios were significantly higher than those for the similarly sized 19.5-kDa FL-dextran (0.56±0.03, n=8), suggesting that passive diffusion might not account for the observed nuclear presence of CaM. Electroporation of 6ROX-CaM into HeLa cells, in the presence of an increased EGTA concentration of 10 mM, gave a F_{np}:$F_{cytoplasm}$ ratio of 1.21±0.02 (n=5) (Fig. 4B), not significantly different from the ratio obtained in the presence of 2 mM EGTA. Glial, neuronal and HeLa cells, loaded with 6ROX-CaM and 20 μg/ml WGA in the presence of 2 mM EGTA displayed F_{np}:$F_{cytoplasm}$ ratios of 0.39±0.02 (n=16), 0.33±0.06 (n=6) and 0.23±0.02 (n=17), respectively (Fig. 4A). This indicates a significant decrease in the concentration of 6ROX-CaM in the nucleus and also a facilitated translocation mechanism that is Ca^{2+}-independent.

The addition of 10 μM mTrp peptide – which interacts with CaM in a Ca^{2+}-dependent manner – before electroporation, gave an F_{np}:$F_{cytoplasm}$ ratio of 1.21±0.01 (n=5) (Fig. 4B), confirming the Ca^{2+}-independence of the nuclear entry of 6ROX-CaM.

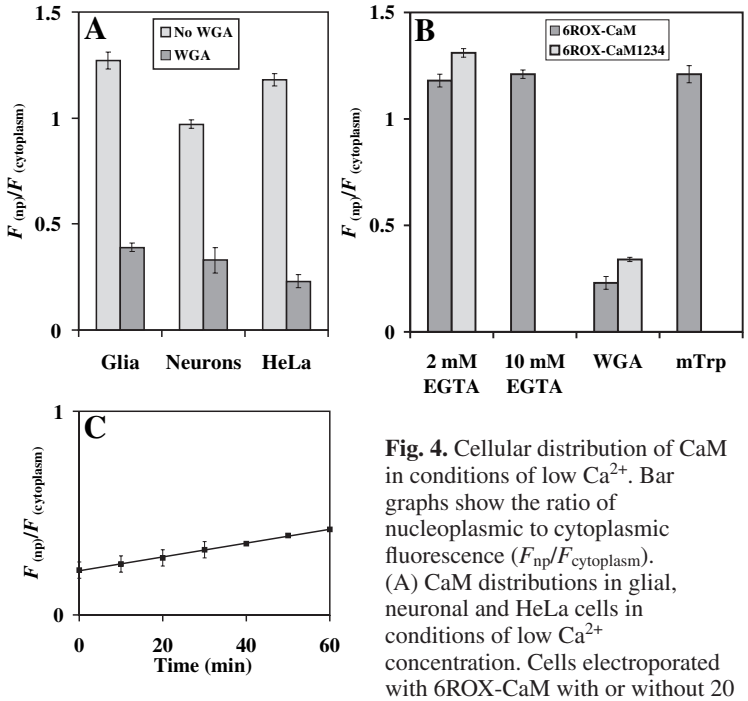

Fig. 4. Cellular distribution of CaM in conditions of low Ca^{2+}. Bar graphs show the ratio of nucleoplasmic to cytoplasmic fluorescence (F_{np}/$F_{cytoplasm}$). (A) CaM distributions in glial, neuronal and HeLa cells in conditions of low Ca^{2+} concentration. Cells electroporated with 6ROX-CaM with or without 20 μg/ml WGA and 2 mM EGTA. (B) HeLa cells, electroporated with 6ROX-CaM and 6ROX-CaM1234 in 2 mM EGTA with or without 20 μg/ml WGA. 6ROX-CaM was also measured after electroporation of 10 mM EGTA instead of 2 mM EGTA. The distribution of 6ROX-CaM is shown in cells incubated with 10 μM mTrp peptide before electroporation (single bar at the right). (C) 6ROX-CaM diffusion rates in low intracellular Ca^{2+} concentration (<10 nM). HeLa cells were electroporated with 6ROX-CaM and with 20 μg/ml WGA in 2 mM EGTA and the F_{np}/$F_{cytoplasm}$ ratio for 6ROX-CaM was recorded for 1 hour.

Passive diffusion of CaM through the nuclear pores at low [Ca^{2+}]

WGA was used to block facilitated entry of 6ROX-CaM into the nucleus in cells that had been electroporated in the presence of 2 mM EGTA. Under these conditions, the rate of change of the F_{np}/$F_{cytoplasm}$ ratio was 0.004±0.0003/min (n=4) (Fig. 4C), similar to that of 19.5-FL-dextran (Fig. 3A).

Ca^{2+}-independent nuclear translocation of 6ROX-CaM1234

Upon loading the cells with 6ROX-CaM1234 in the presence of 2 mM EGTA, the F_{np}:$F_{cytoplasm}$ ratio was 1.31±0.04 (n=15). Cells loaded with 6ROX-CaM1234 and 20 μg/ml WGA in the presence 2 mM EGTA, and imaged 15 minutes after electroporation, displayed a F_{np}:$F_{cytoplasm}$ ratio of 0.34±0.06 (n=9). This was a significant decrease in the concentration of 6ROX-

CaM1234 in the nucleus (Fig. 4B), which indicates a facilitated transport mechanism for CaM that did not require Ca^{2+}.

Ca^{2+}-dependent nuclear translocation of 6ROX-CaM in HeLa cells

Upon stimulation with 2.1 mM Ca^{2+} there was a 1.2- to 1.3-fold increase in 6ROX-CaM fluorescence throughout the cell. This can be explained by the sensitivity of 6ROX-CaM fluorescence to Ca^{2+} as shown in Fig. 1G. There was also strong association of the 6ROX-CaM with the nucleoli from 6ROX-CaM already in the nucleoplasm, which was particularly noticeable in HeLa and glial cells. So, Ca^{2+} stimulation probably induced immediate binding of 6ROX-CaM that was present in the nucleoplasm before stimulation.

Typically there was a delay of up to 40 seconds in the translocation of 6ROX-CaM to the nucleus from the cytoplasm compared to that of Ca^{2+}, which was also noted by Craske et al. (Craske et al., 1999). The time to reach half-maximum fluorescence ($t_{1/2}$) of 6ROX-CaM translocation was 80±12 seconds (n=12). The F_{np}:$F_{cytoplasm}$ ratio showed a significant increase from 1.11±0.04 (t_0) to 1.63±0.05 (t_{317}) and the nucleolic-cytoplasmic fluorescence ratio had markedly increased from 0.92±0.04 to 2.8±0.2. The fluorescence of 6ROX-CaM in the cytoplasm after 317 seconds was also significant and the measured relative fluorescence dropped from 1 to 0.68±0.04. An example of Ca^{2+}-dependent nuclear translocation of 6ROX-CaM in a HeLa cell is shown in Fig. 5 (a representative Ca^{2+} signal is shown below in Fig. 8D).

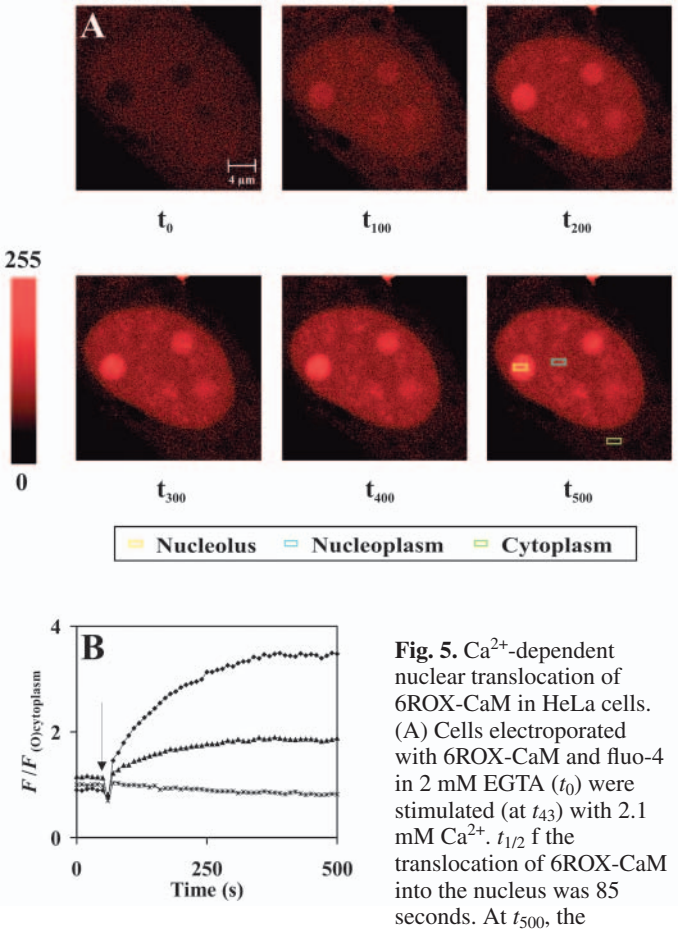

Fig. 5. Ca^{2+}-dependent nuclear translocation of 6ROX-CaM in HeLa cells. (A) Cells electroporated with 6ROX-CaM and fluo-4 in 2 mM EGTA (t_0) were stimulated (at t_{43}) with 2.1 mM Ca^{2+}. $t_{1/2}$ f the translocation of 6ROX-CaM into the nucleus was 85 seconds. At t_{500}, the concentration of 6ROX-CaM that was associated with nucleoli and was present in the nucleoplasm had increased 3.9-fold and 1.7-fold, respectively. Nuclear translocation of 6ROX-CaM was measured at 0, 100, 200, 300, 400 and 500 seconds (t_0 to t_{500}) and the data are shown in (B). Colored boxes indicate areas that have been measured for nuclear translocation of 6ROX-CaM. (B) Time course of the normalized 6ROX-CaM fluorescence ($F/F_{(O)cytoplasm}$) in the (◆) nucleolus, (▲) nucleoplasm and (*) cytoplasm. The arrow indicates the addition of 2.1 mM Ca^{2+}.

Ca^{2+}-dependent nuclear translocation of 6ROX-CaM in cortical glial cells

Similarly to HeLa cells, stimulation of electroporated glial

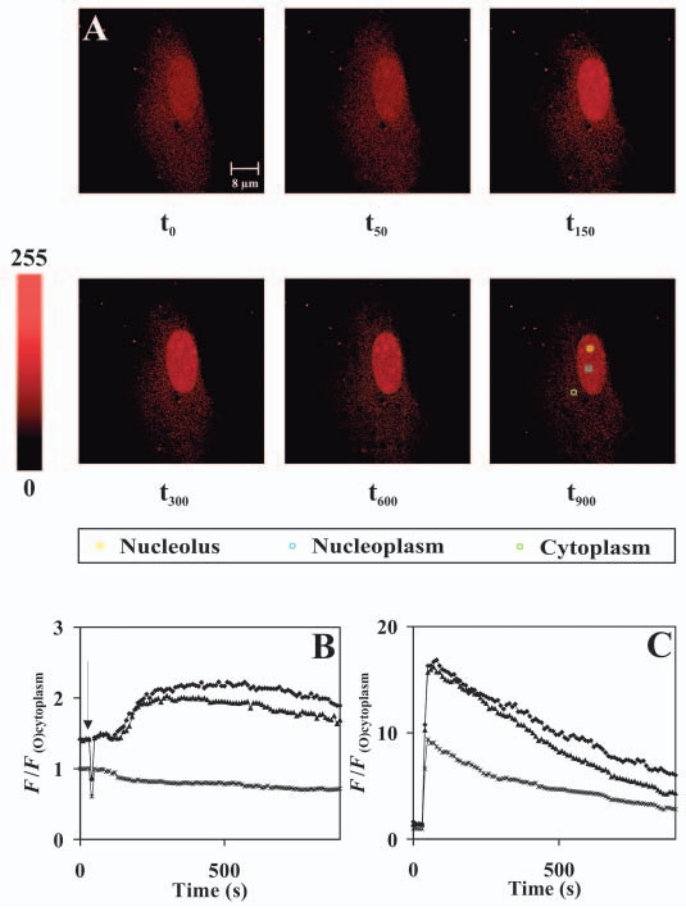

Fig. 6. Ca^{2+}-dependent nuclear translocation of 6ROX-CaM in glial cells (A) Glial cell electroporated with 6ROX-CaM and fluo-4 in 2 mM EGTA (t_0). Cells were stimulated with 2.1 mM Ca^{2+} at t_{50}. $t_{1/2}$ of the translocation of 6ROX-CaM into the nucleus was 40 seconds. At t_{300} seconds, the concentration of 6ROX-CaM associated with nucleoli and in the nucleoplasm had increased 1.5-fold and 1.4-fold, respectively. Nuclear translocation of 6ROX-CaM and fluo-4 was measured at 0, 50, 150, 300, 600 and 900 seconds (t_0 to t_{900}) and the respective data are shown in (B and C) Colored boxes indicate areas that have been measured for nuclear translocation of 6ROX-CaM and fluo-4. (B) Time course of normalized 6ROX-CaM fluorescence ($F/F_{(O)cytoplasm}$) in the (◆) nucleolus, (▲) nucleoplasm and (*) cytoplasm. The arrow indicates the addition of 2.1 mM Ca^{2+}. (C) Time course of intracellular free Ca^{2+} concentration changes monitored by fluo-4 normalized fluorescence ($F/F_{(O)cytoplasm}$) in the same area of the cell as 6ROX-CaM in B.

cells with 2.1 mM Ca^{2+} caused 6ROX-CaM-binding to nucleoli and translocation completed with a $t_{1/2}$ of 82±18 seconds (n=5). The F_{np}:$F_{cytoplasm}$ ratio showed a significant increase from 1.27±0.03 (t_0), to 1.8±0.12 (t_{282}). The nucleolic-cytoplasmic fluorescence had also significantly increased within 282 seconds from 1.23±0.06 to 2.02±0.04. The decrease in 6ROX-CaM fluorescence in the cytoplasm was also significant, with its relative fluorescence dropping from 1 to 0.75±0.06 within 282 seconds. An example of Ca^{2+}-dependent nuclear translocation of 6ROX-CaM and the Ca^{2+} signal monitored by fluo-4 fluorescence in a glial cell is shown in Fig. 6.

Ca^{2+}-dependent nuclear translocation of 6ROX-CaM in cortical neurons

The addition of 2.1 mM Ca^{2+} to neurons electroporated with 6ROX-CaM, caused nuclear translocation of 6ROX-CaM and was completed with a $t_{1/2}$ of 90±20 seconds (n=4). The F_{np}:$F_{cytoplasm}$ ratio showed a significant increase from 0.97±0.02 (t_0) to 1.7±0.2 (t_{290}). The relative fluorescence of 6ROX-CaM in the cytoplasm, 290 seconds after stimulation, decreased from 1 to 0.82±0.13. Fig. 7 shows 6ROX-CaM nuclear translocation and a representative Ca^{2+} signal monitored by fluo-4 in a cortical neuron.

Inhibition of Ca^{2+}-dependent nuclear translocation of 6ROX-CaM by mTrp

The cell-permeant peptide mTrp was added to the cells to inhibit Ca^{2+}-dependent nuclear translocation. HeLa cells were electroporated with 6ROX-CaM and left for 15 minutes in electroporation buffer supplemented with 10 μM mTrp peptide (n=7). In these cells, the addition of 2.1 mM Ca^{2+} into the extracellular medium caused no Ca^{2+}-dependent nuclear translocation or binding of 6ROX-CaM to nucleoli, even though a normal Ca^{2+} transient was observed (Fig. 8A-D).

Inhibition by mAIP

AIP is a potent inhibitor of CaMKII and has been reported to be highly specific (Ishida et al., 1995). AIP also prevented Ca^{2+}-dependent nuclear translocation of 6ROX-CaM in HeLa cells, even though a normal Ca^{2+} transient was observed (n=15). This suggested that CaMKII is responsible for the translocation of CaM into the nucleus, either by acting as a carrier or by phosphorylating CaM. However, myristoylated (mAIP) prevented 6ROX-CaM from binding to nuclear targets in about 80% of the cells tested. This was surprising and suggested that mAIP directly interacts with CaM, in a way similar to mTrp. TA-CaM in 100 μM Ca^{2+}, 100 mM KCl, 2 mM $MgCl_2$ and 50 mM K-MES pH 7.0 at 21°C was thus titrated with mAIP in a fluorimetric assay. Additions of mAIP up to 140 nM caused a 1.67-fold increase in TA-CaM fluorescence. A K_d value of 68 nM was obtained by numerical fitting to the data. However, in the presence of 2 mM EGTA there was no increase in TA-CaM fluorescence upon addition of up to 140 nM mAIP. This indicated that mAIP can interact with TA-CaM in a Ca^{2+}-dependent manner (Fig. 8E).

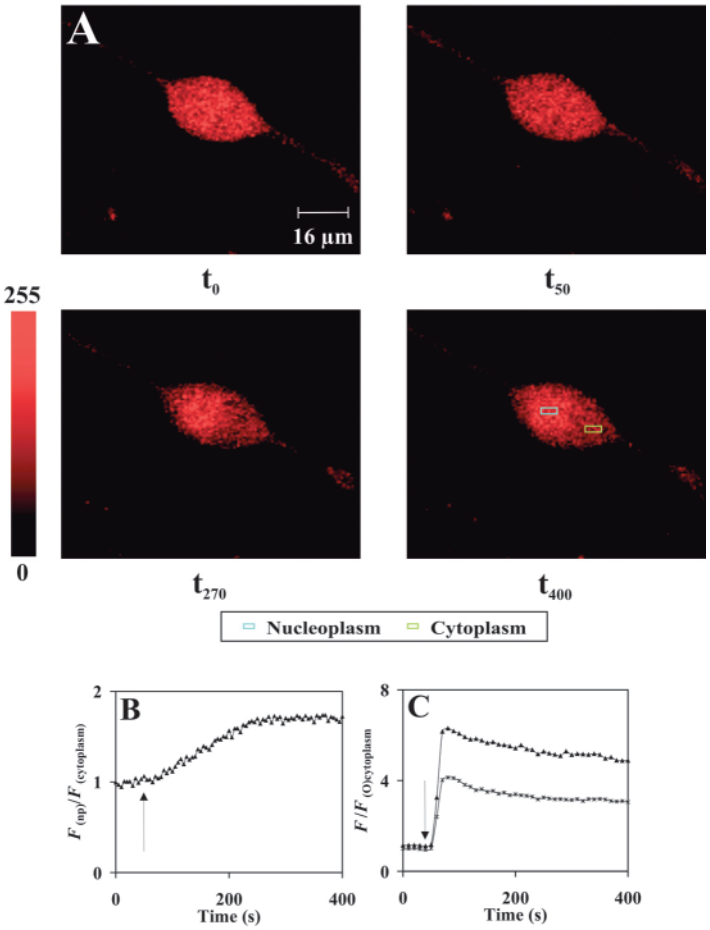

Fig. 7. Ca^{2+}-dependent nuclear translocation of 6ROX-CaM in rat cortical neurons. (A) Neurons electroporated with 6ROX-CaM and fluo-4 in 2 mM EGTA (first image, t_0). The cell was stimulated with 2.1 mM Ca^{2+} (t_{50}). $t_{1/2}$ of the translocation of 6ROX-CaM into the nucleus was 90 seconds. At t_{300} seconds, the concentration of 6ROX-CaM associated in the nucleoplasm had increased 1.7-fold. Nuclear translocation of 6ROX-CaM and fluo-4 was measured at 0, 50, 270 and 400 seconds (t_0 to t_{400}) and the respective data are shown in (B and C) Colored boxes indicate areas that have been measured for nuclear translocation of 6ROX-CaM and fluo-4. (B) Time course of the $F_{np}/F_{cytoplasm}$ ratio of 6ROX-CaM and (C) and of the normalized fluorescence ($F/F_{(O)cytoplasm}$) of fluo-4 in a representative record. Arrows indicate 2.1 mM Ca^{2+} addition.

Passive diffusion of CaM through the nuclear pores at elevated intracellular [Ca^{2+}]

Passive diffusion of 6ROX-CaM was measured in HeLa cells that had been stimulated with 2.1 mM Ca^{2+} in the presence of 10 μM mTrp peptide. Under these conditions, the F_{np}:$F_{cytoplasm}$ ratio change was 0.01±0.002/min (n=5) (Fig. 8F). Thus, the rate of diffusion of Ca^{2+}-6ROX-CaM-mTrp was similar to that of FL-dextran (Fig. 3A).

Inhibition of Ca^{2+}-dependent nuclear translocation of 6ROX-CaM by WGA

WGA was electroporated into HeLa, glial and neuronal cells at an estimated final concentration of 20 μg/ml together with

6ROX-CaM or 6ROX-CaM1234, to determine whether CaM entry upon stimulation with 2.1 mM Ca^{2+} was by passive diffusion or by a facilitated mechanism. Upon stimulation there were no significant increases in the F_{np}:$F_{cytoplasm}$ ratios in any of the cells. The rate of change in F_{np}:$F_{cytoplasm}$ of 6ROX-CaM was 0.012/min. This rate was similar to 6ROX-CaM in 10 μM mTrp stimulated with 2.1 mM Ca^{2+} (0.01/min), indicating that even when Ca^{2+}/CaM was free to bind targets in the nucleus, the rate of diffusion into the nucleus was the same as when binding was inhibited by mTrp. Similarly, HeLa cells loaded with 6ROX-CaM1234 showed no immediate nuclear translocation upon Ca^{2+} addition. These results demonstrated that Ca^{2+}-dependent nuclear translocation (like Ca^{2+}-independent nuclear translocation) occurred via a facilitated mechanism and passive diffusion did not play a significant role in either the localization of CaM in cells under resting conditions or in response to stimuli (Fig. 9).

Discussion

We have used novel CaM probes and a membrane-permeant peptide antagonist to determine the Ca^{2+}-dependent and -independent mechanisms of the nuclear transport of CaM. 6ROX-CaM activated PDE similarly to unlabeled, bacterially expressed human liver CaM and, therefore, the 6ROX label had little effect on the ability of 6ROX-CaM to bind to targets.

Previous work on CaM nuclear translocation has produced conflicting results and, as we present here, this is partly because CaM appears to have a multitude of mechanisms regulating its entry to the nucleus. Not fully taken into account by previous reports is the state of the NPCs during CaM translocation. It is well documented that the nuclear pores are in a more-closed state when intracellular Ca^{2+} stores are depleted, preventing a passive diffusion of molecules with a molecular mass >10 kDa (Stehno-Bittel et al., 1995; Perez-Terzic et al., 1999). By using our methods, we found that, in HeLa cells, FL-dextrans with the molecular mass of 9.5-40 kDa were significantly inhibited from passively diffusing into the nucleus. It is, however, not certain whether a closing-up of the nuclear pores was owing to store depletion or a result of considerable Ca^{2+}-buffering in the cell. Neither the application of BAPTA-AM before electroporation nor a higher concentration of EGTA, reduced the F_{np}:$F_{cytoplasm}$ ratio further than the one found with 2 mM EGTA.

Slow store-refilling has been described before (Hofer et al., 1998). In pancreatic acinar cells, acetylcholine (ACh) stimulation kept Ca^{2+} stores depleted as long as the agonist was present. Upon removal of ACh, the concentration of Ca^{2+} in the ER lumen began to rise but did not reach the original levels for minutes. From the results shown here it was probable that significant store-refilling occurred after the addition of 2.1 mM Ca^{2+} to the extracellular medium. It was, however, not possible

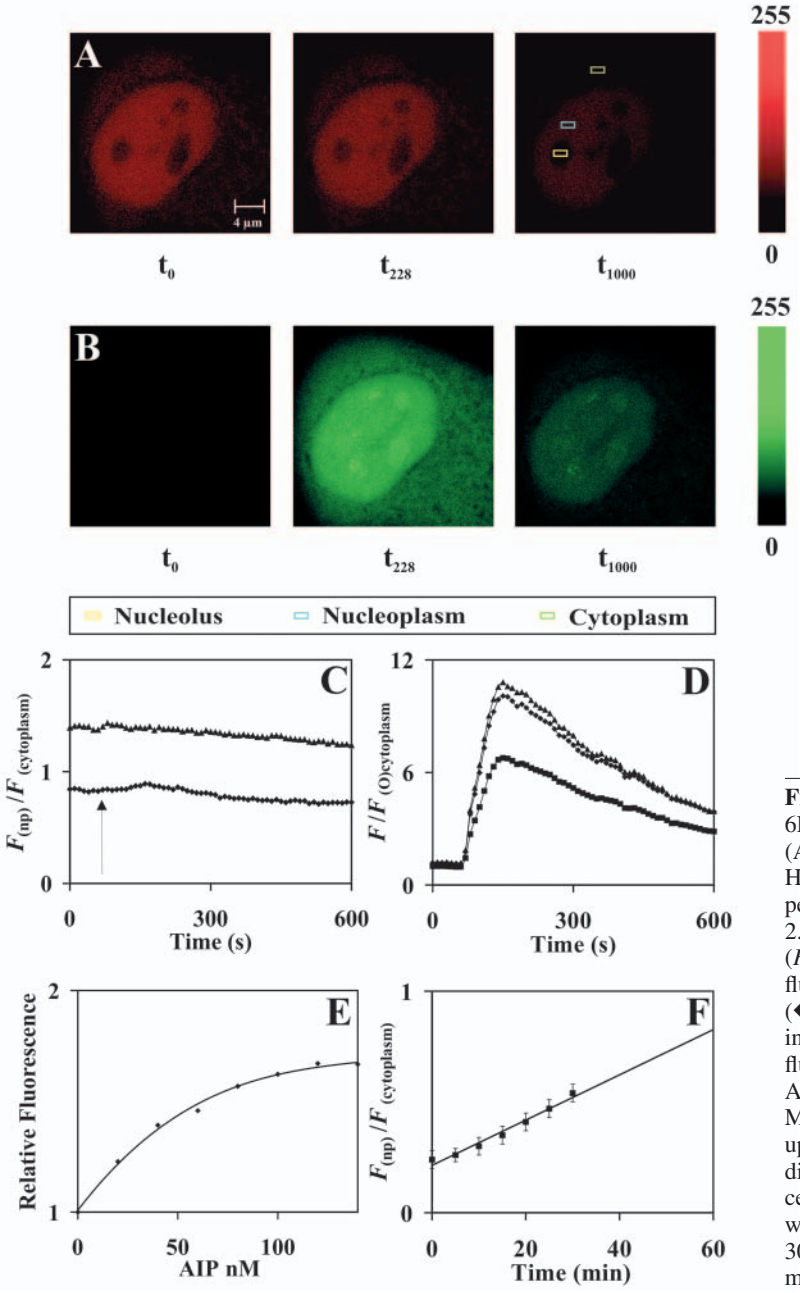

Fig. 8. Inhibition of Ca^{2+}-dependent nuclear translocation of 6ROX-CaM by mTrp peptide in HeLa cells. (A,B) Fluorescence of (A) 6ROX-CaM and (B) fluo-4 in HeLa cells in 2 mM EGTA incubated with 10 μM mTrp-peptide for 15 minutes (t_0). At t_{50} cells were stimulated with 2.1 mM Ca^{2+}. (C,D) Time course of normalized fluorescence ($F/F_{(O)cytoplasm}$) of 6ROX-CaM (C) and normalized fluorescence ($F/F_{(O)cytoplasm}$) of fluo-4 (D) in the nucleolus (◆), nucleoplasm (▲) and cytoplasm (■). Arrow in C indicates the addition of 2.1 mM Ca^{2+}. (E) Relative fluorescence of TA-CaM with increasing concentrations of AIP. A solution of 21 nM TA-CaM, 100 mM KCl, 2 mM $MgCl_2$ and 50 mM K-MES, pH 7.0 at 21°C was titrated with up to 140 nM mAIP in 100 μM Ca^{2+} (◆). (F) 6ROX-CaM diffusion rate at elevated levels of intracellular Ca^{2+}. HeLa cells were electroporated with 6ROX-CaM and stimulated with 2.1 mM Ca^{2+} in the presence of 10 μM mTrp peptide for 30 minutes. The $F_{np}/F_{cytoplasm}$ ratio over a period of 30 minutes was monitored.

to conclude whether store-refilling affected the nuclear pore diameter or whether the direct binding of Ca^{2+} to NPC was sufficient.

Fluo-4 fluorescence was typically higher in the areas around the nucleoli. This phenomenon might originate in the different binding affinities of fluo-4 for subcellular compartments (Thomas et al., 2000). However, it could be related to recently described nuclear tubules or nucleoplasmic reticulum, which either transect the nucleus entirely or terminate near to the nucleoli and are responsible for the release of free Ca^{2+} into the nucleus (Echevarria et al., 2003).

FL-dextran distributions were similar in the three cell types studied. The 4.3-kDa FL-dextran freely entered the nucleus in all conditions. A similar result has been reported with a 3-kDa FL-dextran, which was able to freely diffuse into the nucleus regardless of the intracellular Ca^{2+} levels within the cell (Perez-Terzic et al., 1999). It was concluded that although the pore size was smaller because of reduced intracellular free Ca^{2+} concentrations, smaller molecules could still pass through the nuclear pores unregulated. Previous observations that molecules >60 kDa cannot enter the nucleus via passive diffusion (Weiss, 1998; Allen et al., 2000; Wei et al., 2003) were also seen to be true here. 77-kDa FL-dextran was inhibited from entering the nucleus in the presence or absence of Ca^{2+}, indicating that molecules of this size need an NLS sequence to pass through the NPC. WGA, which blocks NLS-facilitated transport by binding to carbohydrate moieties on nucleoporins did, as expected, not have any effect on the passive diffusion of any FL-dextrans. This has also been seen in rat hepatoma cells using a fluorescently-labeled nucleoplasmin and a 10-kDa dextran (Dabauvalle et al., 1988). In WGA-containing cells, only nucleoplasmin was blocked from entering the nucleus, whereas the dextran was still able to enter. It was concluded that WGA does not constrict the nuclear pore, but binds to O-glycosidically-bound carbohydrates of specific nucleoporins to inhibit facilitated transport.

To observe nuclear translocation of 6ROX-CaM in our experiments, HeLa, glial and neuronal cells were, after electroporation in the presence of EGTA, immersed in an extracellular buffer containing 2 mM EGTA; then 2.1 mM Ca^{2+} was added. Stimulation of nuclear translocation of CaM by Ca^{2+} probably explains the results of Milikan and Bolsover, namely that FL-CaM had a significantly higher F_{np}:$F_{cytoplasm}$ ratio compared with a 10-kDa FL-dextran in micro-injected dorsal root ganglion cells (Milikan and Bolsover, 2000). This was attributed to be a property of the FL-CaM, although it is more probable that there was a Ca^{2+} transient associated with the injection process, which drove the fluorescent CaM into the nucleus. Furthermore, FL-CaM and TA-CaM were found to be localized in the nucleus of resting cells, which were loaded by patch pipettes. However, the cells were washed in a solution of high of [Ca^{2+}], which again – as shown by our data – would have caused an increase of intracellular Ca^{2+} causing nuclear CaM

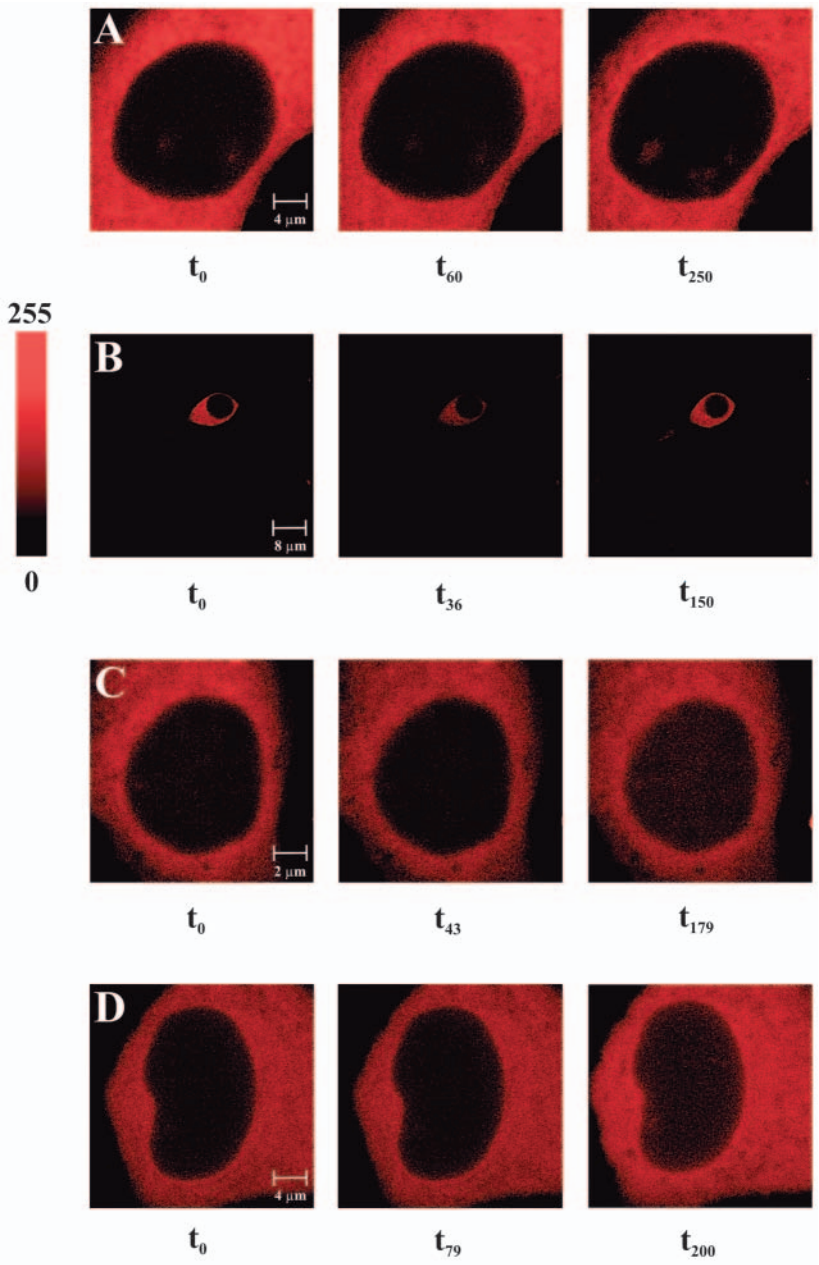

Fig. 9. Inhibition of nuclear translocation by WGA. (A-C) Inhibition of Ca^{2+}-dependent nuclear translocation of 6ROX-CaM in HeLa, neuronal and glial cells by WGA. HeLa cells (A) were electroporated with 6ROX-CaM and 20 µg/ml WGA in 2 mM EGTA (t_0). The cells was stimulated with 2.1 mM Ca^{2+} at t_{60}. A further image, showing inhibition of nuclear translocation, was taken at t_{250}. Neurons (B) were electroporated with 6ROX-CaM and 20 µg/ml WGA in 2 mM EGTA (t_0). The cells were stimulated with 2.1 mM Ca^{2+} at t_{36}. A further image, showing inhibition of nuclear translocation, was taken at t_{150}. Glial cells (C) were electroporated with 6ROX-CaM and 20 µg/ml WGA in 2 mM EGTA (t_0). The cells were stimulated with 2.1 mM Ca^{2+} at t_{43}. A further image, showing inhibition of nuclear translocation, was taken at t_{179}. (D) HeLa cell electroporated with 6ROX-CaM1234 and 20 µg/ml WGA in 2 mM EGTA (t_0). The cell was stimulated with 2.1 mM Ca^{2+} at t_{79}. A further image, showing inhibition of nuclear translocation, was taken at t_{200}.

translocation. Hardingham et al., found endogenous CaM and also microinjected FITC-CaM to be localized in the nucleus of resting hippocampal neurons (Hardingham et al., 2001). Our data show that, whereas the Ca^{2+}-independent mechanism causes an equilibrium of CaM between the cytoplasm and the nucleus, any further nuclear accumulation of CaM requires a Ca^{2+} stimulus. Therefore, the hippocampal neurons were probably stimulated, either by microinjection or a change of extracellular solution, before the experiments to test gene expression were carried out. Nuclear localization was inhibited by WGA, demonstrating that CaM was transported into the nucleus by a facilitated mechanism consistent with this interpretation.

Because passive diffusion of 19.5 kDa-FL-dextran is very slow, 6ROX-CaM, which has an average mass of 17223.1 Da, would be expected to be blocked from entry into the nucleus. However, upon imaging the cells in low Ca^{2+} conditions (<10 nM), the concentration of 6ROX-CaM in the nucleus was similar to that in the cytoplasm. This contrasted the behavior of 19.5-kDa FL-dextran, which was at a significantly lower concentration in the nucleus than in the cytoplasm when the cells were kept in the same conditions. This indicated that 6ROX-CaM was entering the nucleus by using a different mechanism than 19.5 kDa FL-dextran. 6ROX-CaM could enter the nucleus by a facilitated mechanism, possibly by being bound to an NLS-containing transporter molecule, independently of $[Ca^{2+}]$. This hypothesis was supported by our observation that WGA significantly inhibited the entry of 6ROX-CaM in resting cells that were kept in EGTA. A similar observation was made by Pruschy et al., who found that in digitonin permeabilized PtK1 cells, WGA was blocking a fluorescein labeled-CaM in Ca^{2+}-free form and ATP depletion had no effect on CaM import (Pruschy et al., 1994). It was therefore concluded that CaM could be imported into the nucleus by a facilitated mechanism that was independent of ATP. Further evidence that CaM could be bound in apo conditions (in which CaM is expected to be a Ca^{2+}-free form) came from the observations by Luby-Phelps and collegues, who reported that only 5% of total endogenous CaM is unbound in smooth muscle cells at resting intracellular $[Ca^{2+}]$ (Luby-Phelps et al., 1995). In Swiss 3T3 cells, bleaching within the nucleus caused rhodamine-labeled CaM-fluorescence to disappear, which then only reappeared with a slow $t_{1/2}$ of equilibration of 2-3 minutes. However, 4-kDa FL-dextran could not be reduced, suggesting that the nuclear import of CaM was constrained. It was suggested that CaM in the cytoplasm was in a complex with another protein (Luby-Phelps et al., 1985). In HeLa cells before electroporation, the addition of mTrp peptide, which interacts with CaM in a Ca^{2+}-dependent manner, did not alter the F_{np}:$F_{cytoplasm}$ ratios. This also indicates that this process is Ca^{2}-independent. The Ca^{2+}-independence of this process was also shown in HeLa cells electroporated with the mutant CaM1234 labeled with 6ROX, which cannot bind Ca^{2+} (Kasri et al., 2003). Ca^{2+} binding deficiency of the mutant was also demonstrated here by the observation that there was no increase in tyrosine fluorescence upon $[Ca^{2+}]$ titrations, whereas CaM gave a 3-fold increase upon $[Ca^{2+}]$ additions to 1 mM. As with 6ROX-CaM, the nucleus contained a similar concentration of 6ROX-CaM1234 compared with cells that had been electroporated in the presence of 2 mM EGTA; WGA was also found to significantly inhibit its nuclear import.

We have described here a possible Ca^{2+}-independent mechanism by which CaM might enter the cell by binding to an NLS-containing transporter molecule. Stimulation of HeLa and glial cells by increasing extracellular Ca^{2+} levels, immediately caused the 6ROX-CaM already present in the nucleus to strongly bind to the nucleoli. Typically, a delay of up to 40 seconds was seen between the increase of intracellular $[Ca^{2+}]$ and the nuclear translocation of CaM. This is similar to the delay of about 30 seconds following the addition ionomycin to pancreatic acinar cells (Craske et al., 1999). This may be of significance as it might allow the nuclear translocation mechanism to discriminate between brief and prolonged Ca^{2+} signals. Ca^{2+}-dependent nuclear translocation of CaM occurred with a $t_{1/2}$ of 80 seconds, reflecting the rate of transfer of a CaM-transporter complex through the nuclear pores. A similar nuclear translocation time for fluorescein-labeled CaM was seen in pancreatic acinar cells upon ionomycin stimulation, after a 30-second delay, translocation was completed in about 260 seconds (Craske et al., 1999). Teruel et al. also reported that in RBL cells loaded with a fluorescein-labeled CaM and stimulated with ionomycin, nuclear translocation was completed after about 300 seconds. However, they concluded that this was the diffusion of free Ca^{2+}-CaM from the cytoplasm to the nucleus (Teruel et al., 2000).

In our system, the nuclear translocation of CaM upon Ca^{2+} addition could not have been owing to diffusion of free Ca^{2+}-CaM because CaM transport was almost completely blocked by WGA. To test 6ROX-CaM diffusion into the nucleus, rates were either measured at low Ca^{2+} levels and in the presence of WGA or at high Ca^{2+} levels and in the presence of mTrp peptide, to prevent the possibility of free Ca^{2+}/6ROX-CaM being drawn to nuclear targets. This was compared with measurements at high Ca^{2+} levels in the presence of WGA, in which case free Ca^{2+}/6ROX-CaM was able to bind to nuclear targets. As with the 19.5-kDa Fl-dextran, the rate of diffusion into the nucleus was 2.5-fold higher at conditions of elevated $[Ca^{2+}]$ compared with low $[Ca^{2+}]$. The rate of facilitated transport of Ca^{2+}/CaM into the nucleus was, however, 25-fold more rapid than passive diffusion. That the entrance of 6ROX-CaM and 6ROX-CaM1234 into the nucleus can be inhibited by WGA, suggests CaM bound to a transporter molecule with an NLS as the principle mechanism of CaM-entry into the nucleus. Our results contrast with the findings by Liao et al., who suggested that Ca^{2+}/CaM was drawn to nuclear targets and freely diffused into the nucleus from the cytoplasm (Liao et al., 1999). In our case, free diffusion of Ca^{2+}/CaM did not account for the translocation of CaM.

If CaM primarily enters the nucleus by an NLS-facilitated mechanism when nuclear pores are in a more-closed state, the one argument against this is the uncertainty of whether the depletion of intracellular Ca^{2+}-stores prevents NLS-mediated transport as well as passive diffusion. Greber and Gerace certainly showed that it prevented not only passive diffusion but also signal-mediated uptake (Greber and Gerace, 1995), but other reports disagree. Marshall et al. demonstrated that in reconstituted *Xenopus laevis* nuclear envelopes, active nuclear import is independent of Ca^{2+}-pools that can be released by ionophores (Marshall et al., 1997). Furthermore,

Strübing and Clapham found that store depletion by carbachol, thapsigargin or ionomycin had no effect on nuclear translocation of GFP-tagged glucocorticoid receptor (Strübing and Clapham, 1999).

Nuclear entry of CaM in response to a Ca^{2+} signal occurred with $t_{1/2}$ values of approximately 80 seconds and was followed by CaM binding to nuclear targets over minutes. Slow binding might reflect the displacement of endogenous CaM from the target and the nuclear entry might also be limited by dissociation of CaM from cytoplasmic targets (Luby-Phelps et al., 1995). It has been demonstrated that CaM inactivation, following a rapid Ca^{2+}-transient, occurs over a period of a minute (Milikan et al., 2002). The nuclear translocation rate of CaM is thus similar to the lifetime of its activated form. The Ca^{2+}-dependent mechanism of nuclear translocation of CaM demonstrated here, is therefore capable of responding to rapid Ca^{2+} signaling with CaM translocating to the nucleus.

We propose that, CaM entry relies on a facilitated mechanism. The identity of the transporter, however, is still unknown. It has previously been reported that CaMKIIα and CaMKIIβ failed to show any striking redistribution upon depolarization of hippocampal neurons (Deisseroth et al., 1998). However, it was found that KN-93, which inhibits CaM kinases and CaMKKs by preventing CaM binding, also prevented CaM translocation in neurons (Mermelstein et al., 2001). It was suggested that CaM can translocate into the nucleus in a complex with a CaMKK and then phosphorylate and activate CaMKIV to phosphorylate CREB in hippocampal neurons (Mermelstein et al., 2001). KN-93, however, is not entirely specific to CaM kinases (Smyth et al., 2002) The CaM binding peptide M13 also prevented CaM nuclear translocation (Mermelstein et al., 2001). Consistent with that report, we found here that the membrane-permeant mTrp peptide inhibited Ca^{2+}-dependent nuclear translocation and binding of 6ROX-CaM to nucleoli. AIP, however, proved to be less specific than previously thought and thus its inhibitory effect on nuclear translocation and binding of 6ROX-CaM can be explained by its binding to Ca^{2+}/CaM rather than its inhibition of CaMKII.

In addition to the classical NLS-dependent protein import, alternative facilitated-diffusion pathways have now been put forward (Matsubayashi et al., 2001, Whitehurst et al., 2001). Nuclear import of the mitogen-activated protein (MAP) kinase ERK2 occurs without cytosolic factors and ATP, but is inhibited by WGA and was thus thought to be based on direct interaction of ERK2 with nucleoporins, and so was not thought to require an individual import carrier (Dabauvalle et al., 1988; Matsubayashi et al., 2001; Whitehurst et al., 2001).

We demonstrate here that, when the nuclear pores are closed CaM enters the nucleus possibly via two distinct facilitated mechanisms, one Ca^{2+}-independent and the other Ca^{2+}-dependent. This is certainly possible because of the vast number of targets CaM binds to. However, the identities of the transporter/s responsible for CaM translocation independent and dependent of Ca^{2+} are still not known.

This work was supported by the MRC, UK. We are grateful to Nael Nadif Kasri (University of Leuven, Belgium) for the *E. coli* expression plasmid of CaM1234 and for the functional assay of our purified protein.

References

Allen, T. D., Cronshaw, J. M., Bagley, S., Kiseleva, E. and Goldberg, M. W. (2000). The nuclear pore complex: mediator of translocation between the nucleus and cytoplasm. *J. Cell Sci.* **113**, 1651-1659.

Bachs, O., Agell, N. and Carafoli, E. (1994). Calmodulin and calmodulin-binding proteins in the nucleus. *Cell Calcium* **16**, 289-296.

Bootman, M., Niggli, E., Berridge, M. and Lipp, P. (1997). Imaging the hierarchical Ca^{2+} signalling system in HeLa cells. *J. Physiol.* **499**, 307-314.

Craske, M., Takeo, T., Gerasimenko, O., Vaillant, C., Török, K., Peterson, O. H. and Tepikin, A. V. (1999). Hormone-induced secretory and nuclear translocation of calmodulin: oscillations of calmodulin concentration with the nucleus as an integrator. *Proc. Natl. Acad. Sci. USA* **96**, 4426-4431.

Dabauvalle, M. C., Schulz, B., Scheer, U. and Peters, R. (1988). Inhibition of nuclear accumulation of karyophilic proteins in living cells by microinjection of the lectin wheat germ agglutinin. *Exp. Cell Res.* **174**, 291-296.

Deisseroth, K., Heist, E. K. and Tsien, R. W. (1998). Translocation of calmodulin to the nucleus supports CREB phosphorylation in hippocampal neurons. *Nature* **392**, 198-202.

Deisseroth, K., Mermelstein, P. G., Xia, H. and Tsien, R. W. (2003). Signaling from synapse to nucleus: the logic behind the mechanisms. *Curr. Opin. Neurobiol.* **13**, 354-365.

Echevarria, W., Leite, M. F., Guerra, M. T., Zipfel, W. R. and Nathanson, M. H. (2003). Regulation of calcium signals in the nucleus by a nucleoplasmic reticulum. *Nat. Cell Biol.* **5**, 440-446.

Greber, U. F. and Gerace, L. (1995). Depletion of calcium from the lumen of the endoplasmic reticulum reversibly inhibits passive diffusion and signal-mediated transport into the nucleus. *J. Cell Biol.* **128**, 5-14.

Hardingham, G. E., Arnold, F. J. L. and Bading, H. (2001). Nuclear calcium signaling controls CREB-mediated gene expression triggered by synaptic activity. *Nat. Neurosci.* **4**, 261-267.

Hofer, A. M., Fasolato, C. and Pozzan, T. (1998). Capacitative Ca^{2+} entry is closely linked to the filling state of internal Ca^{2+} stores: a study using simultaneous measurements of ICRAC and intraluminal [Ca^{2+}]. *J. Cell Biol.* **140**, 325-334.

Ishida, A., Kameshita, I., Okuno, S., Kitani, T. and Fujisawa, H. (1995). A novel highly specific and potent inhibitor of calmodulin-dependent protein kinase II. *Biochem. Biophys. Res. Commun.* **212**, 806-812.

Kasri, N. N., Sienaert, I., Parys, J. B., Callewaert, G., Missiaen, L., Jeromin, A. and de Smedt, H. (2003). A novel Ca^{2+}-induced Ca^{2+} release mechanism in A7r5 cells regulated by calmodulin-like proteins. *J. Biol. Chem.* **278**, 27548-27555.

Lee, M. A., Dunn, R. C., Clapham, D. E. and Stehno-Bittel, L. (1998). Calcium regulation of nuclear pore permeability. *Cell Calcium* **23**, 91-101.

Li, C., Heim, R., Lu, P., Pu, Y., Tsien, R. Y. and Chang, D. C. (1999). Dynamic redistribution of calmodulin in HeLa cells during cell division as revealed by a GFP-calmodulin fusion protein technique. *J. Cell Sci.* **112**, 1567-1577.

Liao, B., Paschal, B. M. and Luby-Phelps, K. (1999). Mechanism of Ca^{2+}-dependent nuclear accumulation of calmodulin. *Proc. Natl. Acad. Sci. USA* **96**, 6217-6222.

Luby-Phelps, K., Lanni, F. and Taylor, D. L. (1985). Behaviour of a fluorescent analogue of calmodulin in living 3T3 cells. *J. Cell Biol.* **101**, 1245-1256.

Luby-Phelps, K., Hori, M., Phelps, J. M. and Won, D. (1995). Ca^{2+}-regulated dynamic compartmentalization of calmodulin in living smooth muscle cells. *J. Biol. Chem.* **270**, 21532-21538.

Marshall, I. C. B., Grant, T. M. and Wilson, K. L. (1997). Ionophore-releasable lumenal Ca^{2+} stores are not required for nuclear envelope assembly or nuclear protein import in *Xenopus* egg extracts. *Cell Calcium* **21**, 151-161.

Matsubayashi, Y., Fukuda, M. and Nishida, E. (2001). Evidence for existence of a nuclear pore complex-mediated cytosol-independent pathway of nuclear translocation of ERK MAP kinase on permeabilised cells. *J. Biol. Chem.* **276**, 41755-41760.

Mayer, B., Klatt, P., Böhme, E. and Schmidt, K. (1992). Regulation of neuronal nitric oxide and cyclic GMP formation by Ca^{2+}. *J. Neurochem.* **59**, 2024-2029.

Mermelstein, P. G., Deisseroth, K., Dasgupta, N., Isaksen, A. L. and Tsien, R. W. (2001). Calmodulin priming: nuclear translocation of a calmodulin complex and the memory of prior neuronal activity. *Proc. Natl. Acad. Sci. USA* **98**, 15342-15347.

Milikan, J. M. and Bolsover, S. R. (2000). Use of fluorescently labeled

calmodulins as tools to measure subcellular calmodulin activation in living dorsal root ganglion cells. *Pflugers Arch.* **439**, 394-400.

Milikan, J. M., Carter, T. D., Horne, J. H., Tzortzopoulos, A., Török, K. and Bolsover, S. R. (2002). Integration of calcium signals by calmodulin in rat sensory neurons. *Eur. J. Neurosci.* **15**, 661-670.

Perez-Terzic, C., Jaconi, C. M. and Clapham, D. E. (1997). Nuclear calcium and the regulation of the nuclear pore complex. *Bioessays* **19**, 7887-7892.

Perez-Terzic, C., Gacy, A. M., Bortolon, R., Dzeja, P. P., Puceat, M., Jaconi, M., Prendergast, F. G. and Terzic, A. (1999). Structural plasticity of the cardiac nuclear pore complex in response to regulators of nuclear import. *Circ. Res.* **84**, 1292-1301.

Persechini, A., Nancy, D. M. and Kretsinger, R. H. (1989). The EF-hand family of calcium-modulated proteins. *Trends Neurosci*. **12**, 462-467.

Pruschy, M., Ju, Y., Spitz, L., Carafoli, E. and Goldfarb, D. S. (1994). Facilitated nuclear transport of calmodulin in tissue culture cells. *J. Cell Biol.* **127**, 1527-1536.

Smyth, J. T., Abbott, A. L., Lee, B., Sienaert, I., Kasri, N. N., de Smedt, H., Ducibella, T., Missiaen, L., Parys, J. B. and Fissore, R. A. (2002). Inhibition of the inositol trisphosphate receptor of mouse eggs and A7r5 cells by KN-93 via a mechanism unrelated to Ca^{2+}/calmodulin-dependent protein kinase II antagonism. *J. Biol. Chem.* **277**, 35061-35070.

Stehno-Bittel, L., Perez-Terzic, C. and Clapham, D. E. (1995). Diffusion across the nuclear envelope inhibited by depletion of the nuclear Ca^{2+} store. *Science* **270**, 1835-1838.

Strübing, C. and Clapham, D. E. (1999). Active nuclear import and export is independent of lumenal Ca^{2+} stores in intact mammalian cells. *J. Gen. Physiol.* **113**, 239-248.

Teruel, M. N. and Meyer, T. (1997). Electroporation-induced formation of individual calcium entry sites in the cell body and processes of adherent cells. *Biophys. J.* **73**, 1785-1796.

Teruel, M. N., Chen, W., Persechini, A. and Meyer, T. (2000). Differential codes for free Ca^{2+}-calmodulin signals in nucleus and cytosol. *Curr. Biol.* **10**, 86-94.

Thomas, D., Tovey, S. C., Collins, T. J., Bootman, M. D., Berridge, M. J. and Lipp, P. (2000). A comparison of fluorescent Ca^{2+} indicator properties and their use in measuring elementary and global Ca^{2+} signals. *Cell Calcium* **28**, 213-223.

Török, K. and Trentham, D. R. (1994). Mechanism of 2-chloro-(epsilon-amino-Lys_{75})-[6-[4-(*N,N*-diethylamino)phenyl]-1,3,5-triazin-4-yl]calmodulin interactions with smooth muscle myosin light chain kinase and derived peptides. *Biochemistry* **33**, 12807-12820.

Török, K., Wilding, M., Groigno, L., Patel, R. and Whitaker, M. (1998a). Imaging the spatial dynamics of calmodulin activation during mitosis. *Curr. Biol.* **8**, 692-699.

Török, K., Cowley, D. J., Brandmeier, B. D., Howell, S., Aitken, A. and Trentham, D. R. (1998b). Inhibition of CaM-activated smooth-muscle myosin light-chain kinase by CaM-binding peptides and fluorescent (phosphodiesterase-activating) CaM derivatives. *Biochemistry* **37**, 6188-6198.

Török, K., Thorogate, R. and Howell, S. (2002). Studying the spatial distribution of Ca^{2+}-binding proteins. In *Methods in Molecular Biology: Calcium-Binding Protein Protocols, Volume 2: Methods and Techniques* (ed. H. J. Vogel), pp. 383-407. Totowa, NJ: Humana Press.

Tzortzopoulos, A., Best, S. L., Kalamida, D. and Török, K. (2004). Ca^{2+}/calmodulin-dependent activation and inactivation mechanisms of αCaMKII and Thr_{286}-phospho-αCaMKII. *Biochemistry* **43**, 6270-6280.

Wang, H. and Clapham, D. E. (1999). Conformational changes of the situ nuclear pore complex. *Biophys. J.* **77**, 241-247.

Wei, X., Henke, V. G., Strübing, C., Brown, E. B. and Clapham, D. E. (2003). Real-time imaging of nuclear permeation by EGFP in single intact cells. *Biophys. J.* **84**, 1317-1327.

Weiss, C. (1998). Importins and exportins: how to get in and out of the nucleus. *Trends Biochem. Sci*. **23**, 185-189.

Whitehurst, A. W., Wilsbacher, J. L., You, Y., Luby-Phelps, K., Moore, M. S. and Cobb, M. H. (2001). ERK2 enters the nucleus by a carrier-independent mechanism. *Proc. Natl. Acad. Sci. USA* **99**, 7496-7501.

Yu, Y. Y., Chen, Y., Dai, G., Chen, J., Sun, X. M., Wen, C. J., Zhao, D. H., Chang, D. C. and Li, C. J. (2004). The association of calmodulin with central spindle regulates the initiation of cytokinesis in HeLa cells. *Int. J. Biochem. Cell Biol.* **36**, 1562-1572.